# **Advanced Functional Materials**

# Ferroelectric self-poling, switching and crystallinity in BiFeO3 thin films. --Manuscript Draft--

Manuscript Number:	adfm.201600468
Full Title:	Ferroelectric self-poling, switching and crystallinity in BiFeO3 thin films.
Article Type:	Full Paper
Section/Category:	
Keywords:	bismuth ferrite; ferroelectric thin films; domains; imprint; crystallinity
Corresponding Author:	Christianne Beekman Florida State University Tallahassee, UNITED STATES
Additional Information:	
Question	Response
Please submit a plain text version of your cover letter here.  If you are submitting a revision of your manuscript, please do not overwrite your original cover letter. There is an opportunity for you to provide your responses to the reviewers later; please do not add them here.	Please find enclosed our manuscript "Ferroelectric self-poling, switching and crystallinity in BiFeO3 thin films" for publication in Advanced Functional Materials. In this work, we show that the polarization state formed during the growth in a model ferroelectric material acts as "imprint" on the polarization, and that switching away from the preferred as-grown polarization direction necessitates the formation of smaller, more disordered domains and therefore leads to larger strain and crystalline distortions.  We believe this work will be of great importance for a broad range of researchers focusing on current or future applications of polar materials (piezoelectrics, ferroelectrics), in particular using novel materials that are desirable due to their high transition temperatures. Usually, "imprint" in ferroelectrics results from repeated switching leading to an off-set of the polarization-vs-field curves that makes switching difficult (i.e., aging). We here observe and explain a very different phenomenon that occurs in materials with a ferroelectric transition temperature above the growth temperature of thin films. In this case, defects and domain structures are created and "locked in" during the growth, such as to stabilize a particular polarization orientation, which may be a serious detriment for memory devices but a critical advantage where a non-switching polar material is desired (such as piezoelectric actuators, novel photovoltaic or photocatalytic applications). Thus, the results are important to a very broad audience across different areas of applications of polar oxides.  We investigate the effect of such self-poling on the crystallinity and the switching properties of the two polymorphs of BiFeO3 (R' and T') in thin films grown on LaAlO3 substrates with slightly different buffer layers. We chose BiFeO3 as it is an ideal model system due to the amount of information available on its structure and ferroelectric properties. We apply a rather unusual combination of techniques to this investigation: syn

	Sincerely,
	Christianne Beekman
	Assistant Professor, Condensed Matter Physics
	Florida State University
	College of Arts & Sciences Department of Physics
	National High Magnetic Field Laboratory 1800 E Paul Dirac Dr
	Tallahassee FL 32310
Corresponding Author Secondary Information:	
Corresponding Author's Institution:	Florida State University
Corresponding Author's Secondary Institution:	
First Author:	Christianne Beekman
First Author Secondary Information:	
Order of Authors:	Christianne Beekman
	Wolter Siemons
	Miaofang Chi
	Nina Balke
	Jane Howe
	Thomas Z Ward
	Petro Maksymovych
	John D Budai
	Jonathan Z Tischler
	Ruqing Xu
	W Liu
	Hans M Christen
Order of Authors Secondary Information:	
Abstract:	Self-poling of ferroelectric films, i.e., a preferred, uniform direction of the ferroelectric polarization in as-grown samples is often observed yet poorly understood despite its importance for device applications. The multiferroic perovskite BiFeO3, which crystallizes in two distinct structural polymorphs depending on applied epitaxial strain, is well known to exhibit self-poling. We investigate the effect of self-poling on the crystallinity and the switching properties of the two polymorphs of BiFeO3 (R' and T') in thin films grown on LaAlO3 substrates with slightly different La0.3Sr0.7MnO3 buffer layers. We show that the polarization state formed during the growth acts as "imprint" on the polarization and that switching the polarization away from this self-poled direction can only be done at the expense of the sample's apparent crystalline uniformity. We observe a fully reversible reduction of the monoclinic domain size; hence, the crystalline uniformity is restored when the polarization is switched back to its original orientation. This is a direct consequence of the growth taking place in the polar phase (below Tc). Switching the polarization away from this configuration, in which defects and domain patterns synergistically minimize the system's energy, leads to a domain state with smaller (and more highly strained and distorted) monoclinic domains.

DOI: 10.1002/((please add manuscript number))

**Article type: Full Paper** 

Title: Ferroelectric self-poling, switching and crystallinity in BiFeO<sub>3</sub> thin films.

Author(s), and Corresponding Author(s)\* C. Beekman, \*1,a, W. Siemons, M. Chi, N. Balke, J.Y. Howe<sup>1,b</sup>, T.Z. Ward, P. Maksymovych, J.D. Budai, J.Z. Tischler, R. Xu, W. Liu, and H.M. Christen\*1,2

((Optional Dedication))

Dr. C. Beekman, <sup>1,a</sup> Dr. W. Siemons, <sup>1</sup> Dr. M. Chi<sup>1</sup>, Dr. J.Y. Howe<sup>1,b</sup>, Dr. T.Z. Ward, <sup>1</sup> Dr. J.D. Budai, <sup>1</sup> and Dr. H.M. Christen<sup>1</sup>

<sup>1</sup>Materials Science and Technology Division, Oak Ridge National Laboratory, Oak Ridge, TN, 37831, **USA** 

<sup>a</sup> Now at Florida State University Physics Department, and National High Magnetic Field Laboratory, Tallahassee, FL 32310, USA

<sup>b</sup> Now at Hitachi High-Technologies Canada Inc., Toronto ON M9W 6A4, Canada

E-mail: christenhm@ornl.gov

E-mail: beekman@magnet.fsu.edu

Dr. N. Balke<sup>2</sup>, Dr. P. Maksymovych<sup>2</sup>, H.M. Christen

<sup>2</sup> Center for Nanophase Materials Science, Oak Ridge National Laboratory, Oak Ridge, TN, 37831, **USA** 

Dr. J.Z. Tischler,<sup>3</sup> Dr. R. Xu,<sup>3</sup> Dr. W. Liu,<sup>3</sup>

<sup>3</sup>Advanced Photon Source, Argonne National Laboratory, Argonne, IL, 60439, USA.

Keywords: ferroelectric thin films, bismuth ferrite, imprint, domains, crystallinity

Self-poling of ferroelectric films, i.e., a preferred, uniform direction of the ferroelectric polarization in as-grown samples is often observed yet poorly understood despite its importance for device applications. The multiferroic perovskite BiFeO<sub>3</sub>, which crystallizes in two distinct structural polymorphs depending on applied epitaxial strain, is well known to exhibit self-poling. We investigate the effect of self-poling on the crystallinity and the switching properties of the two polymorphs of BiFeO<sub>3</sub> (R' and T') in thin films grown on LaAlO<sub>3</sub> substrates with slightly different La<sub>0.3</sub>Sr<sub>0.7</sub>MnO<sub>3</sub> buffer layers. We show that the polarization state formed during the growth acts as "imprint" on the polarization and that switching the polarization away from this self-poled direction can only be done at the expense of the sample's apparent crystalline uniformity. We observe a fully reversible reduction of the

monoclinic domain size; hence, the crystalline uniformity is restored when the polarization is switched back to its original orientation. This is a direct consequence of the growth taking place in the polar phase (below Tc). Switching the polarization away from this configuration, in which defects and domain patterns synergistically minimize the system's energy, leads to a domain state with smaller (and more highly strained and distorted) monoclinic domains.

## 1. Introduction

A well-established phenomenon in ferroelectric materials and devices is that of self-poling, i.e., a preferred uniform direction of the ferroelectric polarization in as-grown samples. This phenomenon is ubiquitous but not well understood and it is often detrimental to device functionality. One of the main issues caused by self-poling is that of retention loss (i.e. backswitching), [1] which seriously impairs the reliability of ferroelectric capacitors. [2-7] A tell-tale sign of such self-poling or "imprint" is a horizontal shift in the hysteresis loop of the ferroelectric switching process. [8, 9] These shifts are observed in a range of ferroelectric materials and are mainly attributed to the presence of uncompensated charges. [10] For example, charges can accumulate at ferroelectric-electrode interfaces due to fatigue/aging [11-16] or they can be induced by introducing charged defects (i.e. Bi or O vacancies) [17, 18] thermally or optically. [19, 20] Furthermore, it has been shown that simply applying mechanical stress by bending PbZrTiO<sub>3</sub> films can lead to elastic switching and to imprint caused by strain gradients (i.e. flexoelectric effect). [21] Hence, charge and strain are very important parameters that determine the severity of self-poling in a wide range of ferroelectric materials. Obtaining a better understanding of imprint is crucial in fabricating improved ferroelectric devices.

In this paper we explore how self-poling affects the ferroelectric switching properties and the monoclinic domain configuration in strained films of multiferroic BiFeO<sub>3</sub>. In the bulk, the crystal structure is rhombohedral with a remnant polarization of 96  $\mu$ C/cm<sup>2</sup>.<sup>[22]</sup> Epitaxial films are monoclinically distorted when grown onto substrates that lead to moderately

# WILEY-VCH

compressive or tensile strains. For films grown on SrTiO<sub>3</sub> (i.e. under weak compressive strain), the structure is rhombohedral with a small monoclinic distortion (R'). [23] When grown under large compressive strain, such as by coherent or nearly-coherent growth onto LaAlO<sub>3</sub> (LAO) substrates, BiFeO<sub>3</sub> forms a monoclinic structure with a large ratio (~1.25) between the out-of-plane (c<sub>pc</sub>) and the in-plane (a<sub>pc</sub>, b<sub>pc</sub>) lattice parameters (where "pc" denotes the pseudocubic notation); [24-26] we refer to this polymorph as T'. In this form, BiFeO<sub>3</sub> has a large predicted<sup>[22]</sup> and experimentally confirmed<sup>[27,28]</sup> polarization (~150 μC/cm<sup>2</sup>). The T<sub>C</sub> for both T' BiFeO<sub>3</sub> (as extrapolated from Raman data<sup>[26]</sup>) and R' BiFeO<sub>3</sub> thin films is around 1100  $K^{[29,30]}$ . For films grown on LAO substrates and thicknesses exceeding ~ 20 nm, strain resulting from thermal-expansion differences between the film and substrate lead to the (reversible) formation of a complex phase coexistence (stripe patterns) when the sample is cooled below 300 °C, and these stripes can be created, moved, and erased using the electric field from a scanning probe. [24, 26, 31-33] The monoclinic majority of these films is made up of 4 symmetry-equivalent structural domain variants, and thus 8 possible polarization directions, each having both an in-plane and an out-of-plane component, as is the case for any polar monoclinic material grown on a square lattice. As mentioned above, high-quality films are typically self-poled such that an as-grown sample exhibits only one direction of the vertical polarization component, i.e. only 4 of the possible 8 polarization orientations are present. According to current literature it appears that when BiFeO<sub>3</sub> is grown on La<sub>0.3</sub>Sr<sub>0.7</sub>MnO<sub>3</sub> (LSMO), the polarization points primarily towards the LSMO electrode both for R' and T' BiFeO<sub>3</sub>. [27,28,34,35] Interestingly, we find that our T' and R' thin films (both grown on LAO substrates under the same nominal growth conditions, as discussed below) reproducibly show opposite preferred polarization directions with respect to one another, which confirms the common assumption that the origin of self-poling (but not necessarily its impact on switching) is strongly dependent on details of sample fabrication. Here we characterize switched regions in our samples using atomic force and piezoresponse force microscopy (AFM and PFM),

transmission electron microscopy (TEM) and synchrotron microdiffraction to determine local crystallographic information. Surprisingly, we find that switching the polarization away from the ferroelectric "self-poling direction" established during growth leads to a reversible reduction in apparent crystallinity, which is defined by the thickness of the film (i.e., reduced x-ray diffraction peak intensities as a consequence of a domain pattern that is associated with large strains, smaller domains, and stronger structural distortions) of both the majority T' polymorph and the R' polymorph; the apparent crystallinity (i.e., diffraction peak intensity) is fully restored when the polarization is switched back to the as-grown direction. We find that the specific conditions of the growth surface are very important in determining the strain state and the morphology of the thin films. The strain and hence the monoclinic domain configuration vary locally across the samples resulting in a spatially varying strength of the imprint. The ability to clear or screen the trapped charges at the film substrate interface and perhaps at the monoclinic domain walls is extremely important in determining the response of the film to the ferroelectric switching process.

#### 2. Results and Discussion

Figure 1 shows AFM topography images for the two types of films investigated here. It is important to emphasize that both the T' phase BiFeO<sub>3</sub> thin film and the R' BiFeO<sub>3</sub> thin film are grown on a LSMO backelectrode on a LAO substrate. Slight variations in growth conditions for the 10 nm thick LSMO layers are most likely the cause for the difference in strain state of the two films. The T' film shows the typical phase coexistence (i.e. stripes embedded in the T' like majority phase) of highly strained BiFeO<sub>3</sub> films<sup>[24, 26, 28,30-32]</sup> and the R' film shows the typical square island growth. The difference in growth morphology for two films of the same composition and grown under the same nominal growth conditions is striking and shows an interesting link between epitaxial strain and surface morphology. Reference films of BiFeO<sub>3</sub> on SrTiO<sub>3</sub> grown in our laboratory (data not shown) show a morphology that is similar to the R' BiFeO<sub>3</sub> on LSMO on LAO films

presented here. In Fig. 1 we also show the  $\theta$ -2 $\theta$  scans that confirm that R' and T' are the majority polymorphs of the two films, respectively, with clear finite size fringes visible for the T' film indicating thickness uniformity. The small amount of intensity at  $2\theta = 22.3^{\circ}$  in the T' film is a diffraction peak of the LSMO, i.e., there is no detectable R' phase in this film. Figure 2 displays STEM – High Angle Annular Dark Field (STEM-HAADF) images of both films. In these atomically resolved images it is clearly seen that the Fe occupies a noncentrosymmetric position with respect to the Bi sublattice (Figure 2 c), i.e. both R' and T' thin films exhibit self-poling. In agreement with the PFM data discussed below, the high resolution TEM images show that the as-grown ferroelectric polarization direction, which is determined during growth, is opposite for the two films; in the T' film the polarization points predominantly towards the substrate (i.e. the Fe-ions are displaced upward, see Figures 2a and c (top)) and for the R' film the polarization points predominantly away from the substrate (i.e. the Fe-ions are displaced downward, see Figure 2 b and c (bottom)). Although a preferred out-of-plane polarization is commonly reported, the direction of the as-grown polarization is not always specified in published reports but is most often observed to point towards the bottom electrode. Contrary to ferroelectrics with a T<sub>c</sub> below the growth temperature, where a domain pattern is formed after growth and under a condition of limited ionic charge mobility, these films are grown in the polar phase. Thus, there is an intricate interplay between polarization and surface termination, as small charges that naturally exist at the surface of the bottom electrode can dominate the polarization of the material as it nucleates, and domain energetics may result in accumulation of charges at specific locations (to screen polar field) – with ionic motion being potentially high at the growth temperature under low-oxygen pressure conditions.

It is well known that a PFM can be used to locally switch the polarization in R' and T' BiFeO<sub>3</sub> thin films. For both samples PFM was used to reverse the polarization with respect to the as-grown direction and subsequently a smaller square was poled back towards the as-

grown polarization direction. To accomplish this, we have applied voltages of +/-8V while scanning the tip across the sample surface to write the ferroelectric domain patterns shown in Figure 3. Here we note that the PFM measurements confirm the observation from TEM in that for the as-grown regions the polarization directions for the R' and T' film are indeed opposite. For both samples the out-of-plane PFM images (amplitude and phase) of the poled regions are shown in Figures 3 (a, b and d, e). Since it is impossible to pole macroscopic regions in these samples, typical sizes of poled areas are only a few tens of microns across. Therefore, we used x-ray synchrotron microdiffraction, [36] a technique that is uniquely suited, to investigate how the structural properties change as the ferroelectric polarization is switched away from the self-poled direction. We identified the 005<sub>pc</sub> peaks of the T'-phase and the R'phase and we subsequently monitored the diffraction peak intensities of these peaks while scanning the beam across the poled regions at fixed (monochromatic) x-ray energy (i.e., at fixed d-spacing). Surprisingly, we find that for both R' and T' films, the regions that are poled away from the as-grown polarization direction show lower diffraction peak intensity compared to the as-grown region, but the regions that were poled twice (i.e., back into the asgrown direction) showed recovered diffraction intensity. This contrast is clearly visible in the area maps of the 005<sub>pc</sub> diffraction peak intensity measured at fixed energy shown in Figure 3 c and f. To clarify the reason for the reduced intensity at fixed Q (the measured intensity is sensitive to the sharpness of the Bragg peak but also to slight changes in lattice orientations), we performed Q-scans (i.e., energy scans) through the 005<sub>pc</sub> diffraction peaks on the as-grown regions, the region that is poled once and the region that is poled twice for both samples. These scans are shown in **Figure 4**. Clearly, switching the polarization away from the selfpoled direction established during growth results in a peak that is broadened in Q and with a reduced intensity for both T' and R' thin films (i.e. crystallinity is reduced and multiple lattice parameters coexist). There is likely an additional broadening in ω, as the integrated intensity over the Q-region is also reduced; however, the experimental conditions of the icrodiffraction

experiment aren't conducive to scans in that direction. Upon switching the polarization back into the as-grown direction the peak intensity and hence the crystallinity are almost fully restored, i.e. this process is largely reversible. Hence, both films are self-poled and can be switched away from that original direction only at the expense of the sample's apparent crystallinity.

When discussing the origin of the changed intensity, we need to note that the T' film is not structurally uniform, the presence of the striped phase (comprised of tilted T' and tilted S' polymorphs)<sup>[26]</sup> definitely results in a weaker T'(005<sub>pc</sub>) majority phase diffraction peak. Furthermore, switching the polarization leads to changes in the amount of stripes in that region as is obvious from the PFM amplitude image in Figure 3. However, the apparent contrast in crystallinity observed using microdiffraction cannot solely be explained by the creation and erasing of the stripes, since the R' film also shows this behavior. This is most strongly demonstrated by the fact that for both the T' and the R' films the contrast in crystallinity of the poled regions remained when the samples were heated to 250 °C (see supplemental information), i.e., a temperature for which most of the striped-phase in the T' film disappears. [26] The reversible change in apparent crystallinity upon switching must therefore be related to the monoclinic domains that exist both in the R' and the T' majority phase. Indeed, focusing for the moment on the T' film, PFM confirms that the majority phase (i.e. the flat areas showing unit cell high terraces) consists of four monoclinic domains as evident from two different stripe orientations and three different contrast levels in the PFM image, [37] and allows us to determine the domain sizes in the film (see **Figure 5**). We find that the as-grown T' BFO has stripe-like monoclinic domains with average length of about 1 µm with the domain walls pointing along the (110)LAO direction consistent with observations by others in a variety of BiFeO<sub>3</sub> thin films.". [38-40] Interestingly, we found that both the striped phase and the monoclinic domain walls are visible in low voltage SEM images as well (Figure 5 d). In situ heating study in the SEM showed that the stripes disappeared during heating and

# WILEY-VCH

reappeared after cooling down to near room temperature. This is particularly interesting as the surface corrugation accompanying them is too small to lead to this contrast. Therefore, changes in electronic conductivity and/or work function may accompany the domain walls (as would be expected, for example, for charged domain walls), or large local discontinuities of the polarization may lead to contrast (see the supporting information for more details on the SEM measurements). To investigate the domain structure further, we turn to in-plane PFM images taken on the T' film on which we again poled a square (5 x 5 µm) away from the as grown polarization and subsequently a smaller square (2x2 µm) within this poled region back into the as-grown polarization direction (see **Figure 6**). We find typical domain configurations and sizes for the as-grown area (compare to Figure 5c). However, when the polarization is forced away from the as- grown preferred direction, the monoclinic domains appear to be greatly reduced in size compared to the as-grown regions. In fact, in this sample they become too small to be observed with our PFM. When switched back to the as-grown direction the monoclinic domains are as large as or perhaps somewhat larger than in the asgrown regions (see Figure 6 b). This clearly shows that switching the polarization away from the self-poling direction leads to a reversible reduction in average size of the monoclinic domains that make up the T' majority phase, which in turn leads to the reduced x-ray diffraction intensity. We note that the voltage necessary for switching the polarization is somewhat location dependent: This is emphasized in **Figure 7** in which we show butterfly loops recorded on a 5 x 5 grid across a scan area of 1.5x 1.5 µm. We show three typical loops to represent the full data set of 25 loops. The figure clearly shows that there is a horizontal shift in all loops, i.e. switching the polarization away from the as-grown direction requires a higher voltage than switching it back, a behavior typically referred to as "imprint" when observed as a consequence of repeated switching.

To understand the origin of these behaviors – the off-set switching loops, the change in apparent crystallinity, and the reduction in domain size – we again consider the fact that these films are grown in the polar phase, i.e., below T<sub>c</sub> for this material. This leads to some very fundamentally different behaviors than what is expected for materials such as BaTiO<sub>3</sub> or PZT that are typically grown in the paraelectric phase. In these latter cases, a domain pattern emerges as the material is cooled through the transition temperature, and the domain configuration is such as to minimize the electrostatic and elastic energies, typically in the absence of mobile charges. For BiFeO<sub>3</sub> it is known that ultrathin films are tetragonal <sup>[41]</sup>, and therefore we can assume that during the growth of the first few monolayers, a tetragonal material is formed. Adsorbed species at the surface of the LSMO electrode (i.e., the surface onto which BiFeO<sub>3</sub> nucleates), oxygen vacancies in the LSMO and in BiFeO<sub>3</sub>, and adsorbed species at the top surface of the BiFeO<sub>3</sub> film, can easily result in a uniformly poled material (the effects of chemically absorbed species at the surface of a film on its polarization orientation are well reported in the literature [42, 43]). Thus, it is likely that a defect structure is created at the electrode/ferroelectric interface that favors a specific polarization direction, and this defect structure will persist during polarization reversal. While it is difficult to estimate how many defects (and what type of defects) are required to fully stabilize a uniformly preferred polarization orientation during growth, the off-sets in the switching data of Fig. 7 indicates that a voltage of ~1V is required to overcome their effect. Upon further growth of BiFeO<sub>3</sub> beyond the initial tetragonal layer, a monoclinic material forms with a domain pattern that minimizes the electrostatic and elastic energies of its domains on a square lattice. Four monoclinic domains (as observed in these samples) cannot coexist with strictly charge-neutral domain walls, which may explain why the domain structure is readily visible in SEM images. However, there is clearly an energetic advantage to incorporate at least some charged defects that help screen the electrostatic energy of some of the domain walls. Upon polarization reversal with a scanning tip, these trapped charges are likely to remain immobile, and the

system will not be allowed to find an equally favorable domain configuration as was created during growth and incorporation of these defects. It is therefore not surprising that a domain structure with smaller domains, and possibly broader, more poorly defined domain walls, will form. The resulting large internal strain variations then lead to the decrease in apparent crystallinity (as observed by the reduced x-ray diffraction intensity in these switched regions).

#### 3. Conclusion

In summary, thin films of BiFeO<sub>3</sub> have a clear self-poling direction that is determined by the specific substrate, bottom electrode and film conditions during growth (in our case, pointing towards the film surface in the case of an R' film grown on LSMO/LAO, and towards the bottom electrode for the T' film on a slightly different LSMO/LAO. Switching the polarization away from this self-poled direction can only be done at the expense of the sample's apparent crystallinity (i.e. significant changes in the local strain distribution corresponding to a changed monoclinic domain configuration). The reduced apparent crystallinity, in the form of a large reduction of the monoclinic domain size, is fully reversible; hence almost full recovery of the crystallinity is observed when the polarization is switched back. This behavior can be attributed to defects that are incorporated during the growth of this polar material to minimize its electrostatic and elastic energy – defects that may be present at the electrode/ferroelectric interface and within the ferroelectric, i.e., at domain walls. Switching away from this pre-formed state is therefore unfavorable, requires a higher voltage than switching back to it, and results in larger structural distortions. Understanding such behavior is crucial for the formation of ferroelectric memory devices based on this highly promising material, as it may negatively affect switching. Conversely, stable prepoling may be of technological benefit for piezoelectric applications or future uses of ferroelectrics in photovoltaics or for applications in electro- or photo-catalysis.

## 4. Experimental Section

The experiments were performed on BiFeO<sub>3</sub> films grown by pulsed laser deposition (PLD) on LAO substrates. The films were grown in a 25 mTorr oxygen background pressure while the substrates were kept at a temperature of 675 °C. A pulsed KrF excimer laser with a wavelength of 248 nm was focused on a 10% excess Bi BiFeO<sub>3</sub> sintered pellet with an energy density of 0.4 J/cm<sup>2</sup> and operated at 2 Hz, resulting in an average deposition rate of ~0.03 Å/pulse. We compare two samples in this work that have the same nominal composition (BiFeO<sub>3</sub> on LSMO on LAO), where the LSMO layer acts as bottom electrode for ferroelectric switching and piezoresponse measurements. The T' sample is obtained by growing a sufficiently thin layer of LSMO for it to be coherently strained to the LAO substrate, thus imposing the same strain state on the BiFeO<sub>3</sub> film as the bare substrate would. This strain coupling across the bottom electrode is highly dependent on the deposition parameters of the LSMO film, with minute variations in film thickness or surface morphology immediately resulting in strain relaxation, i.e. formation of R' BiFeO<sub>3</sub> on a nominally identical (or highly similar) LSMO electrode. This allows us to compare R' and T' films both grown on LAO substrates. Characterization of the films was done through synchrotron x-ray microdiffraction, which was performed at beamline 34-ID-E at the Advanced Photon Source at Argonne National Laboratory[44], with  $0.5 \times 0.5 \ \mu m^2$  beam focal size, 45° fixed incidence angle, and tunable photon energy from 7 to 30 keV. AFM images were taken on a Veeco D3100 operated in tapping mode. The PFM measurements were performed on the same Veeco Dimension Nanoscope equipped with external lock-in amplifiers. Using conducting AFM tips we measured the local electrical and topographical properties simultaneously and independently. For the out-of-plane PFM imaging, a single frequency ac bias of 2V close to the contact resonance frequency of the tip-sample contact was applied to the tip and the PFM amplitude and phase were recorded. For poling, a dc voltage of +/- 8V was applied to the scanning tip which was sufficient to reverse the orientation of the ferroelectric domains

without inducing irreversible topographic changes (i.e. sample destruction). For the in-plane PFM measurements we used the band-excitation method to avoid crosstalk with the surface topography. The method allows mapping of the resonance frequency, local quality factor and response amplitude (amplitude-based feedback is used to track the cantilever resonance and quality factor). The switching loops were taken in ultrahigh vacuum using an Omicron VT-SPM modified for piezoresponse force microscopy. All the vacuum experiments were carried out at pressures better than  $5 \times 10^{-9}$  Torr using Pt-coated conducting AFM tips (Budget Sensors ElectriMulti75). The labscale x-ray diffraction (XRD) reciprocal space mapping (RSM) was performed on a laboratory PanAlytical X'Pert thin film diffractometer with Cu K $\alpha$  radiation. The TEM characterization was carried out on an FEI-Titan 60/300 microscope at the operation voltage of 300 kV. TEM specimens were prepared using mechanical polishing, followed by low-voltage (2 kV) cryo ion-milling. SEM study was undertaken using a Zeiss Merlin SEM at 0.7 kV accelerating voltage. The SEM specimen was prepared by back-thinning of the LAO film to 20  $\mu$ m.

## **Supporting Information**

Supporting Information is available from the Wiley Online Library or from the author.

## Acknowledgements

Research supported by the U. S. Department of Energy (DOE), Basic Energy Sciences (BES), Materials Science and Engineering Division (HMC, JDB, WS, CB, TWZ, MC and JH), and performed in part (PFM and SEM measurements) at the Center for Nanophase Materials Science, which is a DOE Office of Science User Facility that also supported NB and PM. X-ray microdiffraction (JZT, RX, WL) was done at the Advanced Photon Source, a U.S. Department of Energy (DOE) Office of Science User Facility operated for the DOE Office of Science by Argonne National Laboratory under Contract No. DE-AC02-06CH11357. A

special thanks to Julia Luck for her extraordinary work in TEM and SEM specimen preparation.

Received: ((will be filled in by the editorial staff))

Revised: ((will be filled in by the editorial staff))

Published online: ((will be filled in by the editorial staff))

[1] A. Gruverman, B. J. Rodriguez, A. I. Kingon, and R. J. Nemanich, J. S. Cross and M. Tsukada, *Appl. Phys. Lett.*, **2003**, 82, 3071.

- [2] R. D. Pugh, M. J. Sabochick, and T. E. Luke, J. Appl. Phys., 1992, 72, 1049
- [3] J. Lee, R. Ramesh, V. G. Keramidas, W. L. Warren, G. E. Pike, and J. T. Evans Jr, *Appl. Phys. Lett.*, **1995**, 66, 1337.
- [4] J. Lee and R. Ramesh, Appl. Phys. Lett., 1996, 68, 484.
- [5] W. L. Warren, B. A. Tuttle, D. Dimos, G. E. Pike, H. N. Al-Shareef, R. Ramesh, and J. T. Evans, Jr., Jpn. J. Appl. Phys., 1996, 35, 1521.
- [6] J. Lee, C. H. Choi, B. H. Park, T. W. Noh, and J. K. Lee, *Appl. Phys. Lett.*, **1998**, 72, 3380.
- [7] K. Knakao, Y. Judai, M. Azuma, Y. Shimada, and T. Otsuki, *Jpn. J. Appl. Phys.*, 1998, 37, 5203.
- [8] Y. Zhou, H. K. Chan, C. H. Lam, and F. G. Shin, J Appl. Phys. 2005, 98, 024111
- [9] W. L. Warren, H. N. Al-Shareef, D. Dimos, B. A. Tuttle, and G. E. Pike, *Appl. Phys. Lett.*, **1996**, 68, 1681.
- [10] M. B. Okatan and S. P. Alpay, Appl. Phys. Lett. 2009, 95 092902
- [11] Michael Grossmann, Oliver Lohse, Dierk Bolten, Ulrich Boettger and Rainer Waser *MRS Proceedings*, **2001** 688, C3.4.1 doi:10.1557/PROC-688-C3.4.1.

- [12] Tagantsev, A. K., Stolichnov, I., Colla, E. L. & Setter, J. Appl. Phys. 2001, 90, 1387.
- [13] Lou, X. J. Appl. Phys. 2009,105, 024101.
- [14] de Araujo, C., Cuchiaro, J. D., McMillan, Scott, M. C. & Scott, J.F. *Nature* **1994** 374,627.
- [15] Lou, X., Zhang, M., Redfern, S. A. T. & Scott, J. F. Phys. Rev. B 2007, 75, 224104.
- [16] Lou, X., Zhang, M., Redfern, S. A. T. & Scott, J. F. Phys. Rev. Lett. 2006, 97, 177601
- [17] Xiaomin Chen, Yuhong Zou, Guoliang Yuan, Min Zeng, J. M. Liu, Jiang Yin and
- Zhiguo Liu J. Am. Ceram. Soc., 2013, 96, 3788.
- [18] M. Alexe, C. Harnagea, D. Hesse, and U. Gosele, Appl. Phys. Lett. 2001, 79 242
- [19] W. L. Warren, D. Dimos, G. E. Pike, B. A. Tuttle, M. V. Raymond, R. Ramesh, and J. T.
- Evans Jr, Appl. Phys. Lett., 1995, 67, 866.
- [20] D. Dimos, W. L. Warren, M. B. Sinclair, B. A. Tuttle, and R. W. Schwartz, J. Appl.
- *Phys.*, **1994**, 76, 4305.
- [21] A. Gruverman, B. J. Rodriguez, A. I. Kingon, and R. J. Nemanich, A. K. Tagantsev,
- J. S. Cross and M. Tsukada Appl. Phys.Lett. 2003, 83 728
- [22] A. J. Hatt, N. A. Spaldin, and C. Ederer, Phys. Rev. B 2010, 81, 54109.
- [23] H.W. Jang, D. Ortiz, S.H. Beak, C.M. Folkman, R.R. Dias, P. Schafer, Y.B. Chen, C.T.
- Nelson, X.Q. Pan, R. Ramesh, and C.B. Eom., Adv. Mater. 2009, 21, 817.
- [24] R.J. Zeches, M.D. Rossell, J.X. Zhang, A.J. Hatt, Q. He, C.H. Yang, A. Kumar, C.H.
- Wang, A. Melville, C. Adamo, G. Sheng, Y.H. Chu, J.F. Ihlefeld, R. Erni, C. Ederer, V.
- Gopalan, L.Q. Chen, D.G. Schlom, N.A. Spaldin, L.W. Martin, and R. Ramesh, *Science* 2009,
- 326, 977.
- [25] H. Béa, B. Dupé, S. Fusil, R. Mattana, E. Jacquet, B. Warot-Fonrose, F. Wilhelm, A.
- Rogalev, S. Petit, V. Cros, A. Anane, F. Petroff, K. Bouzehouane, G. Geneste, B. Dkhil, S.
- Lisenkov, I. Ponomareva, L. Bellaiche, M. Bibes, and A. Barthélémy, *Phys. Rev. Lett.* 2009,
- 102, 217603.

- [26] C. Beekman, W. Siemons, T.Z. Ward, M. Chi, J. Howe, M.D. Biegalski, N. Balke, P.
- Maksymovych, A.K. Farrar, J.B. Romero, P. Gao, X. Pan, D.A. Tenne, and H.M. Christen,

Adv. Mater. 2013, 25, 5561

[27] M. D. Rossell, R. Erni, M. P. Prange, J.-C. Idrobo, W. Luo, R. J. Zeches, S. T.

Pantelides, and R. Ramesh, *Phys. Rev. Lett.* **2012**, 108, 047601.

- [28] J. X. Zhang, Q. He, M. Trassin, W. Luo, D. Yi, M. D. Rossell, P. Yu, L. You, C. H.
- Wang, C.Y. Kuo, J. T. Heron, Z. Hu, R. J. Zeches, H. J. Lin, A. Tanaka, C. T. Chen, L. H.
- Tjeng, Y.-H. Chu, and R. Ramesh, *Phys. Rev. Lett.* **2011**, 107, 147602.
- [29] D Sando, A. Barthelemy and M. Bibes, J. Phys.: Condens. Matter **2014**, 26, 473201
- [30] W Siemons, C Beekman, G J MacDougall, J L Zarestky, S E Nagler and H M Christen, J.
- Phys. D: Appl. Phys. **2014**, 47, 034011
- [31] A. R. Damodaran, C. W. Liang, Q. He, C. Y. Peng, L. Chang, Y. H. Chu and L. W.
- Martin, Adv. Mater. 2011, 23, 3170.
- [32] Y. C. Chen, Q. He, F. N. Chu, Y. C. Huang, J. W. Chen, W. I. Liang, R. K. Vasudevan,
- V. Nagarajan, E. Arenholz, S. V. Kalinin and Y. H. Chu, Adv. Mater. 2012, 24, 3070.
- [33] N. Balke, S. Choudhury, S. Jesse, M. Huijben, Y. H. Chu, A. P. Baddorf, L. Q. Chen, R.
- Ramesh & S. V. Kalinin Nature Nanotech. 2009, 4, 868
- [34] P. Yu, J.-S. Lee, S. Okamoto, M. D. Rossell, M. Huijben, C.-H. Yang, Q. He, J. X.
- Zhang, S. Y. Yang, M. J. Lee, Q. M. Ramasse, R. Erni, Y.-H. Chu, D. A. Arena, C.-C. Kao, L.
- W. Martin, and R. Ramesh, *Phys. Rev. Lett.* **2010**, 105, 027201.
- [35] S. M. Wu, Shane A. Cybart, P. Yu, M. D. Rossell, J. X. Zhang, R. Ramesh and R. C.
- Dynes, *Nature Mater.* **2010**, 9, 756
- [36] C. Beekman, W. Siemons, T. Z. Ward, J. D. Budai, J. Z. Tischler, R. Xu, W. Liu, N. Balke, J. H. Nam, and H. M. Christen, *Appl. Phys. Lett.* **2013**, 102, 221910
- [37] F. Zavaliche, R. R. Das, D. M. Kim, and C. B. Eom, S. Y. Yang, P. Shafer, and R.
- Ramesh, Appl. Phys. Lett. 2005, 87, 182912

- [38] Z. H. Chen, Y. Qi, L. You, P. Yang, C. W. Huang, J. Wang, T. Sritharan, and L. Chen, *Phys. Rev. B* **2013**, 88, 054114.
- [39] A.A. Bokov and Z.-G. Ye J. Appl. Phys. 2004, 95, 6347
- [40] Z. H. Chen, A. R. Damodaran, R. Xu, S. Lee and L. W. Martin, Appl. Phys. Lett. 2014, 104 182908
- [41] Y. Yang, C. M. Schlepütz, C. Adamo, D. G. Schlom, and R. Clarke, APL Mater. 2013, 1, 052102
- [42] Highland, M.J.; Fister, T.T.; Richard, M.; Fong, D.D.; Fuoss, P.H.; Thompson, C.;
- Eastman, J.A., Streiffer, S.K. Stephenson, G.B. Phys. Rev. Lett. 2010, 105, 167601
- [43] J. Shin, V.B. Nascimento, G. Geneste, J. Rundgren, E.W. Plummer, B. Dkhil, S.V.
- Klinin, and A.P. Baddorf, Nano Letters 2009, 9, 3720
- [44]J.D. Budai, W. Liu, J.Z. Tischler, Z.W. Pan, and D.P. Norton, B.C. Larson, W. Yang, and G.E. Ice *Thin Solid Films* **2008**, 516, 8013
- [45]S. Jesse, S.V. Kalinin, R. Proksch, A P Baddorf and B J Rodriguez Nanotech. 2007, 18
- [46] P. Maksymovych, S. Jesse, M. Huijben, R. Ramesh, A. Morozovska, S. Choudhury, L.-Q. Chen, A. P. Baddorf, S. V. Kalinin, *Phys. Rev. Lett.* **2009**, 102, 017601.

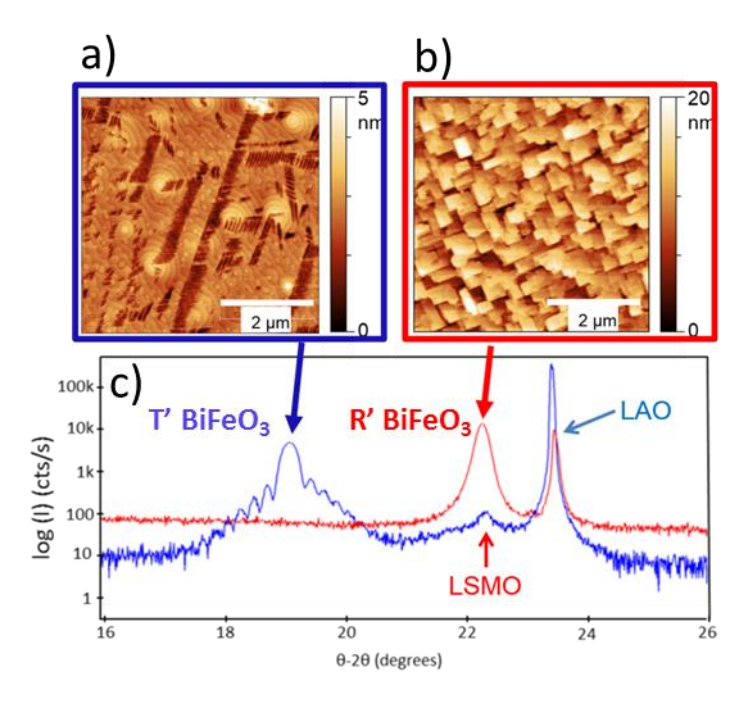


**Figure 1.** a) AFM topography image of a 50 nm thick T' BiFeO<sub>3</sub> film on 10 nm thick LSMO on LAO. Scan size:  $5 \times 5 \mu m$  b) AFM topography image of a 50 nm thick R' BiFeO<sub>3</sub> film on on 10 nm thick LSMO on LAO. Scan size:  $5 \times 5 \mu m$ . c) X-ray  $\theta$ -2 $\theta$  scans for both samples R' (red curve) and T' (blue curve).

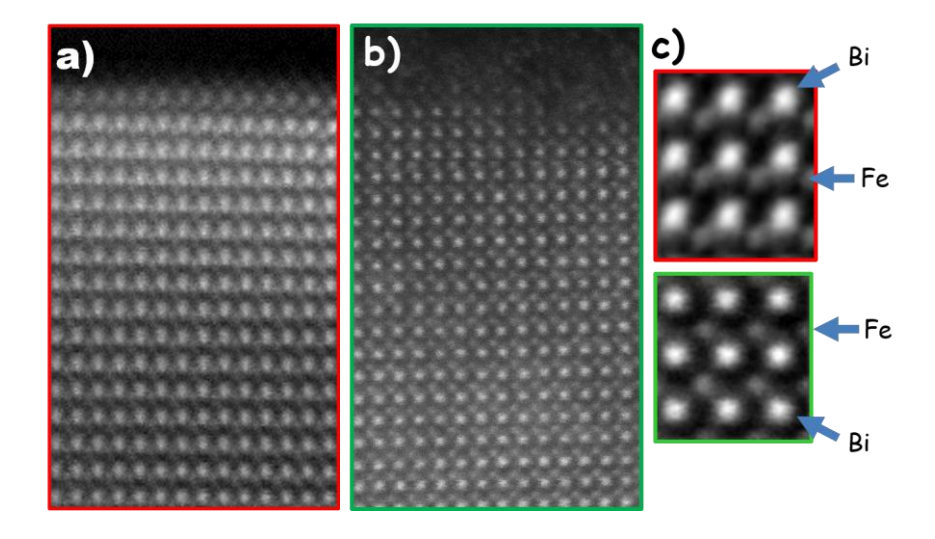


**Figure 2.** STEM-HAADF images at room temperature of the same films shown in Figure 1 taken along the 100 zone axis. a) the T' BiFeO<sub>3</sub> film. b) the R' BiFeO<sub>3</sub> film. c) Magnified images to display the unit cells, top: T' BiFeO<sub>3</sub> and bottom: R' BiFeO<sub>3</sub>. Atomic positions are

indicated by the arrows. The image of the T' film was taken on a region devoid of the stripes that are visible in AFM (Figure 1a).

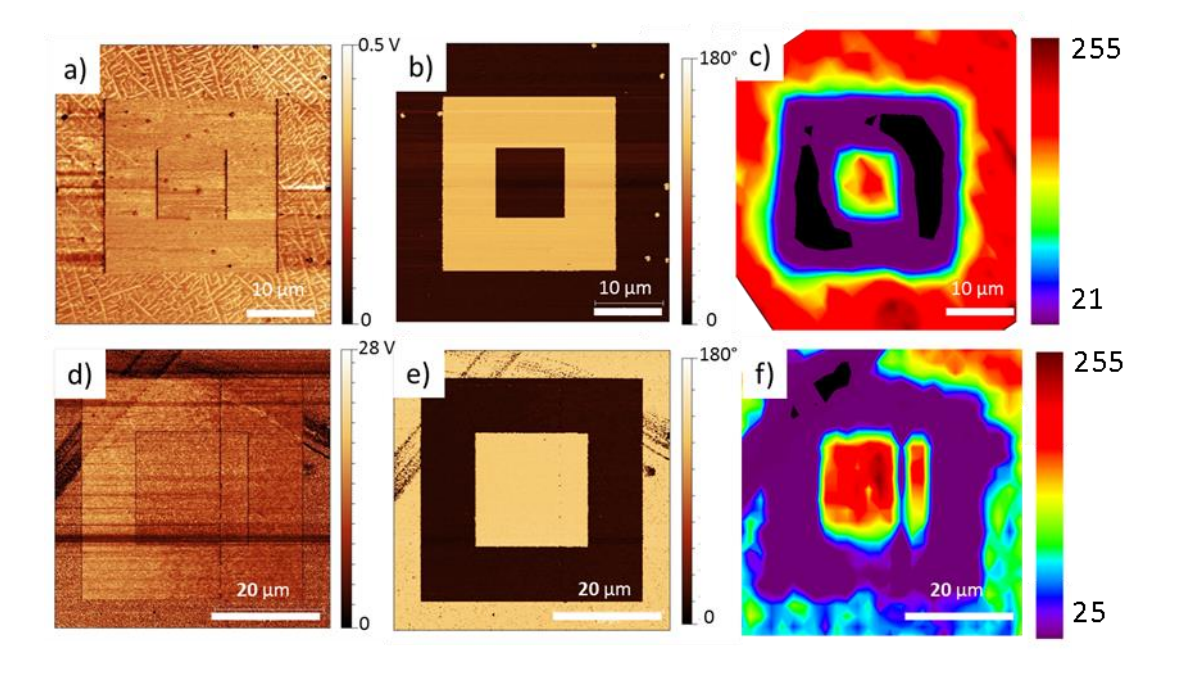


**Figure 3**: Top panels: a) PFM amplitude image on a T' 50 nm BiFeO<sub>3</sub> grown on LSMO bottom electrode on a LAO substrate. b) PFM phase image on the sample shown in a. c) Area map of the total intensity of the T'(005<sub>pc</sub>) BiFeO<sub>3</sub> x-ray diffraction peak measured at fixed energy E = 9.64kV. Bottom panels: d) PFM amplitude image on a R' 50 nm BiFeO<sub>3</sub> grown on LSMO bottom electrode on a LAO substrate. e) PFM phase image on the sample shown in d. f) Area map of the total intensity of the R'(005<sub>pc</sub>) BiFeO<sub>3</sub> diffraction peak measured at fixed energy E = 11.056kV. (Note: these are the same films as in Figures 1 and 2).

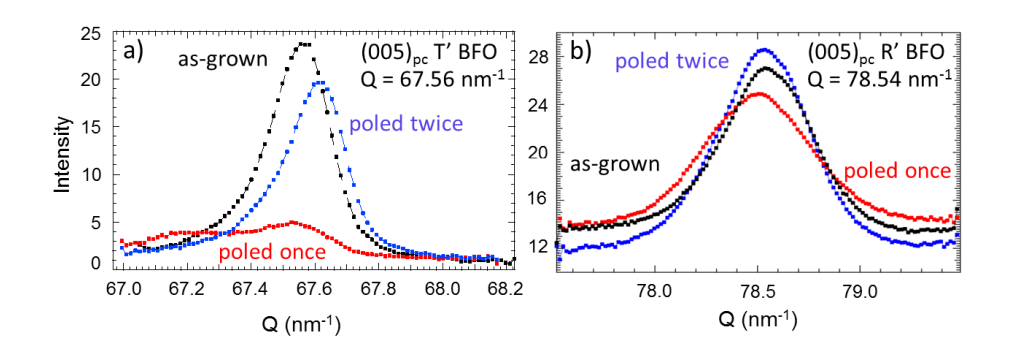


**Figure4** a) Energy scans covering the entire Q-range of a particular diffraction peak. a) Scans through the T'(005) film diffraction peak at three different locations in the switched regions, as-grown (black), poled up (red) and poled back down (blue). b) Scans through the R'(005) film diffraction peak at three different locations in the switched regions, as-grown (black), poled down (red) and poled back up (blue).

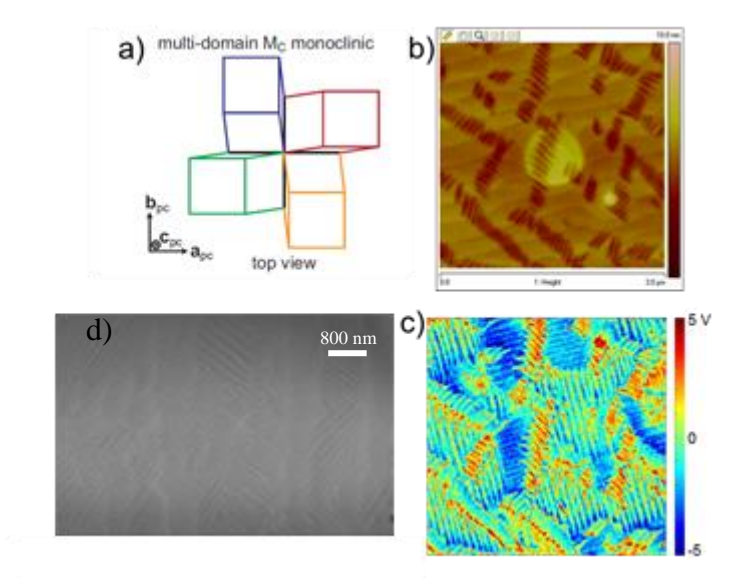


**Figure 5**: a) Schematic showing the structural domains of a monoclinic  $T'(M_C)$  BiFeO<sub>3</sub> thin film. b) AFM image showing the region for which we recorded the PFM signal. c) In-plane PFM signal corresponding to the image shown in b). Scan size: 3 x 3  $\mu$ m. d) SEM image of the BiFeO<sub>3</sub> thin film surface at E = 0.7 kV (beam range 5 nm) taken at room temperature.

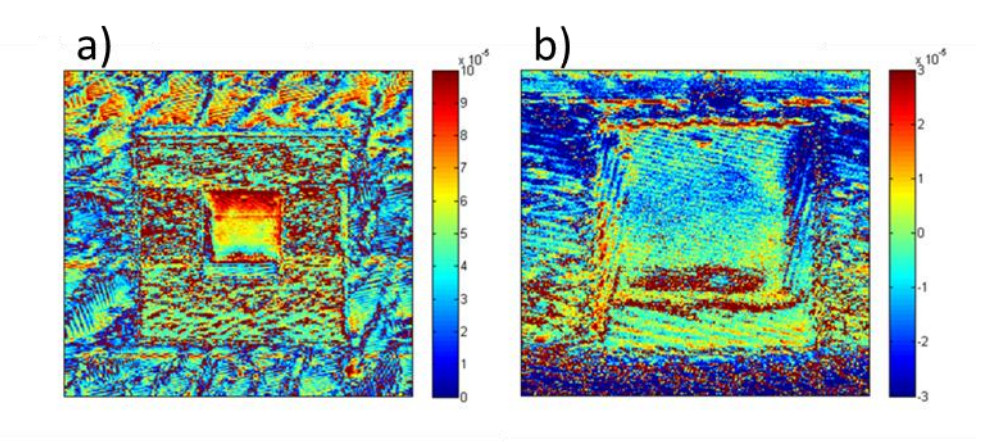


**Figure 6**. In-plane PFM amplitude images of a 50 nm T' BiFeO<sub>3</sub> film. Scan sizes: a)  $8 \times 8 \mu m$  b)  $3 \times 3 \mu m$ . The two images are taken in separate scans. Due to multiple tip-crashes for the image shown in b, it was necessary to substract a fitted baseline to flatten that image. The color scale bars are in volts.

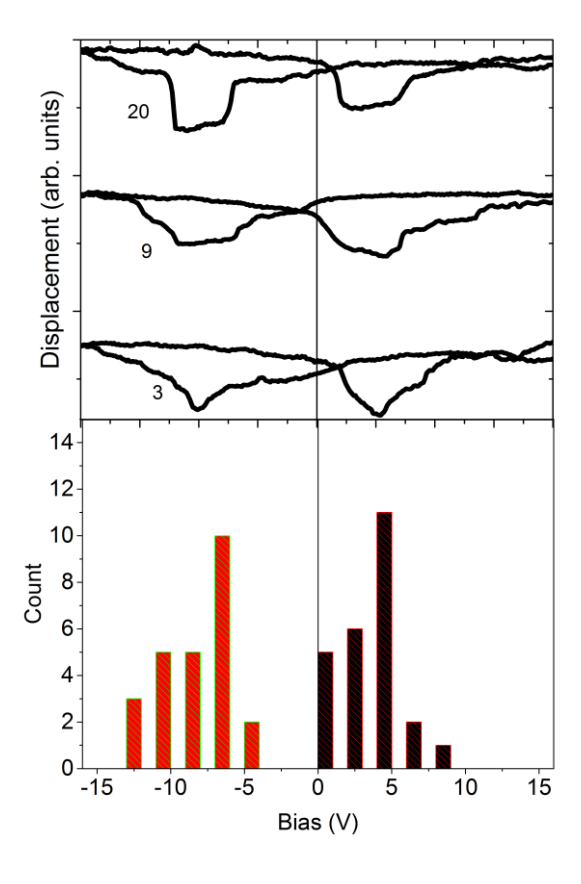


**Figure 7**: (top) Local PFM butterfly loops taken at room temperature on the as-grown T' phase film. The numbers indicate positions in a 5 x 5 grid spanning a 1.5 x 1.5  $\mu$ m scan area. (bottom) histogram of the switching voltages determined from the butterfly loops in the

# WILEY-VCH

measured grid. The switching voltage were either taken as the minimum in the butterfly loops or as an average determined for very broad switching features as for example in loop 20. (see supporting information for details)

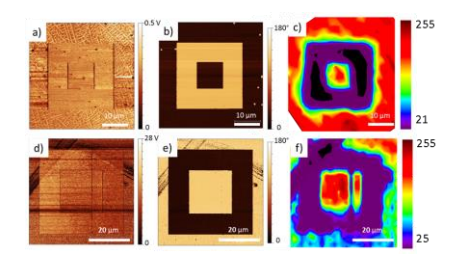
The table of contents entry should be 50–60 words long, and the first phrase should be bold. The entry should be written in the present tense and impersonal style.

## **Keyword**

C. Beekman, W. Siemons, M. Chi<sup>1</sup>, N. Balke<sup>2</sup>, J.Y. Howe<sup>1b</sup>, T.Z. Ward, P. Maksymovych<sup>2</sup>, J.D. Budai, J.Z. Tischler, R. Xu, W. Liu, and H.M. Christen\*<sup>1,2</sup>

Title: Ferroelectric self-poling, switching and crystallinity in BiFeO<sub>3</sub> thin films.

Defects formed and charges trapped during growth at the ferroelectric/electrode interface and within the film determine the lowest energy domain configuration and strain state of BiFeO<sub>3</sub> films. Polarization reversal thus leads to the formation of an energetically less favorable domain and strain state with smaller monoclinic domains and weaker x-ray diffraction intensity.



**Supporting Information** 

Click here to access/download

Supporting Information

Supporting

Information\_udiffmanuscript\_submit\_Jan2016.pdf

Supporting Information

Click here to access/download **Supporting Information** SEM\_heating\_movie.avi